Bollettino di Geofisica Teorica ed Applicata Vol. 53, n. 2, pp. 231-242; June 2012
DOI 10.4430/bgta0056

Non-negative Matrix Factorization: an application to Erta 'Ale volcano, Ethiopia

G. Cabras[1], R. Carniel[2] and J. Jones[3]

[1] *Dipartimento di Chimica, Fisica e Ambiente, Università di Udine, Italy*
[2] *Laboratorio di misure e trattamento dei segnali, DICA, Università di Udine, Italy*
[3] *Dept. of Earth and Space Sciences, University of Washington, Seattle WA, USA*

(Received: July 13, 2011; accepted: December 21, 2011)

ABSTRACT Non-negative Matrix Factorization (NMF) is an emerging new technique in the blind separation of signals recorded in a variety of different fields. The application of these techniques to the analysis of volcanic signals is new to date. Volcanic tremor, the continuous seismic signal recorded close to a volcano, often consists of a mixture of signals having different and independent sources, both volcanic and non-volcanic, possibly including anthropogenic ones. In this paper we show that NMF is a suitable technique to separate such a mixture of foreground / interesting / target "signals" from background / interference / undesired "noise". The encouraging results obtained with this methodology in the presented case study, separating high convection foreground signal from low convection background noise at Erta 'Ale lava lake, support its wider applicability in volcanic signals separation.

Keyword: Non-negative Matrix Factorization, volcanic tremor, lava lake convection regimes, volcanic signal separation.

1. Introduction

Volcanic tremor, recorded at or near an active volcano, often consists of a mixture of signals in a wide, usually overlapping, range of frequency bands. In this paper we discuss the possibility of application of blind techniques to the problem of separating the sources of such signals composing the recorded tremor. This approach is based on the Non-negative Matrix Factorization (NMF) and can be applied to a single-sensor dataset. As an illustrative case study, we analyze data recorded at Erta 'Ale volcano, where NMF is applied in order to separate a relatively transient "high lava lake convection phase" signal from an underlying, relatively continuous, "low lava lake convection phase" signal.

2. Volcanic tremor time series

Studies of volcanic tremor time series have become very common over the last several decades, because of tremor's potential value for better understanding the physical processes that occur inside active volcanoes, and therefore possibly for forecasting eruptions (Lovallo *et al*., 2010). Moreover, the tools developed to analyze volcanic tremor can be applied identically to other kinds of tremor, such as tremor associated with hydrocarbon reservoirs (Dangel *et al*.,

Table 1 - Terms that characterize volcanic tremor in the time or frequency domain (after Konstantinou and Schlindwein, 2002).

Term	Domain	Description	Example
Harmonic	Frequency/Time	Multiple peaks in the spectrum with a fundamental frequency and its harmonics	Mt. Semeru
Monochromatic	Frequency/Time	Spectrum consisting of only one sharp peak extending over a narrow frequency band	Ruapehu
Banded	Time	Tremor bursts separated by periods of quiescence, that resemble stripes or bands on a seismogram	Miyakejima, Etna
Spasmodic	Time	Continuous tremor with large amplitude variations, that probably depend on magma flow or lava fountaining	Krafla
Tremor storm	Time	Small duration tremor bursts superposed on the background earthquake activity	Etna

2003), a subject of great recent research interest, whose detection remains an open problem (Ali *et al*., 2010). Other commonly studied sources of nonvolcanic tremor include geothermal activity (Carniel *et al*., 2010) and plate subduction (Rogers and Dragert, 2003). However, the analysis of volcanic (and non-volcanic) tremor signals and the understanding of the physical mechanisms underlying their generation is a very difficult task.

The term "volcanic tremor", as formally defined by Konstantinou and Schlindwein (2002), refers to a persistent seismic signal observed only near active volcanoes, lasting from several minutes to months or more, preceding or accompanying most volcanic eruptions. At some volcanoes, such as Stromboli (Italy) and Yasur (Vanuatu), tremor has been observed continuously since seismic monitoring began. An entire terminology has been created to characterize the appearance of tremor signals in the time or frequency domain, such as monotonic (or harmonic) or non-monotonic (or non-harmonic) vibrations; Konstantinou and Schlindwein (2002) proposed the terms defined in Table 1.

To investigate the nature of volcanic tremor signals, the amplitude spectrum and spectrogram are fundamental analysis tools. But we have to take into account some important characteristics of tremor signals:

- tremor can persist for long periods of time, resulting in the accumulation of large amounts of data that have to be analyzed;
- they may exhibit strong temporal variations in amplitude and/or frequency content that should be monitored, because of their importance for source modeling and eruption forecasting;
- the calculated spectrum may have multiple sharp peaks around narrow frequency bands (i.e., in monochromatic tremor), in which case a high degree of resolution is required in order to resolve the individual frequencies;
- they often exhibit non volcanic signal contamination, usually dominated by ocean microseisms (Kadota and Labianca, 1981) in the frequency bands 0.1-0.3 Hz and local noise of anthropogenic origin (e.g., industrial activities and human activity in general) in frequencies higher then 1 Hz (Carniel *et al*., 2008).

Removing microseismic or other types of interference is an important stage in processing

volcanic tremor signals and, as pointed out by recent field experiments by Ali *et al*. (2010), similar problems make the detectability of hydrocarbon tremor comparably challenging. In Cabras *et al*. (2008, 2010c), we proposed a methodology based on Blind Source Separation techniques to isolate tremor components of proper volcanic origin from multisensor datasets contaminated by microseisms. In this work, we present a new approach based on Non-negative Matrix Factorization technique to extract a target source from a single-sensor volcanic seismic datasets.

3. Erta 'Ale volcano seismic dataset

Erta 'Ale is a basaltic shield volcano in Afar region, Ethiopia (13.608°N, 40.678°E, 613 m a.s.l.). The volcano features a 1600 x 700 m^2 summit caldera with two pit craters where one or more lava lakes are almost permanently hosted since at least 1906 (Dainelli and Marinelli, 1907; Barberi and Varet, 1970). These constitute the upper surface of a convecting magma column, which allows continuous observations of magma system circulation (Oppenheimer and Francis, 1998) driven by density contrasts that can arise from a combination of degassing, crystallisation and, especially at a superficial level, cooling (Harris, 2008). In February 2002 simultaneous seismic, thermal and video data were acquired by Harris *et al*. (2005) and Alean *et al*. (2011). In particular, a 5 s Lennartz LE-3D, a 30 s Guralp CMG-40 and a 0.5 s Mark Products L-22 seismometer were used, together with an Omega thermal infrared thermometer. Harris *et al*. (2005) mainly studied the thermal signal to track convection processes in the lake, while Jones *et al*. (2006) focused on the continuous, non monochromatic, volcanic tremor, to investigate the variable rates of lava lake convection. The lake cycled between tens-of-minutes-long periods characterized by low (0.01 – 0.08 m/s) and high (0.1 – 0.4 m/s) convection rates. The seismic signature of each regime was characterized by Jones *et al*. (2006) using spectral content, wavefield polarization, and tremor source location. In his Ph.D. work, Jones (2009) suggested that continuous tremor had multiple, simultaneously active seismic sources, not all of which were persistent: magma flow in a conduit, degassing at fumaroles, gas bubbles coalescing in the shallow, active lava lake, and degassing in a crater that formerly held a lava lake. The spectral transitions result from secondary signals introduced during periods of rapid lava lake convection. The signal, which we interpret as being generated by magma flow in a conduit, does not change between the two convective regimes. Thus, changes in the rate of lava lake convection (and corresponding spectral changes) are driven entirely by shallow processes in the lava lake, rather than changing properties of the magma supply. The separation of a "high convective" seismic source of interest from a "low convective" non stationary noise in a single-sensor seismic time series recording is a challenging task that, if successful, could be extended to other seismic noise time series.

4. A novel approach to single-sensor seismic analysis

The presented approach is implemented by the Non-negative Matrix Factorization (NMF), where the basic idea is that we can obtain a meaningful part-based factor decomposition (Lee and Seung, 1999) from a single-channel data observation by the only constraints of non-negativity

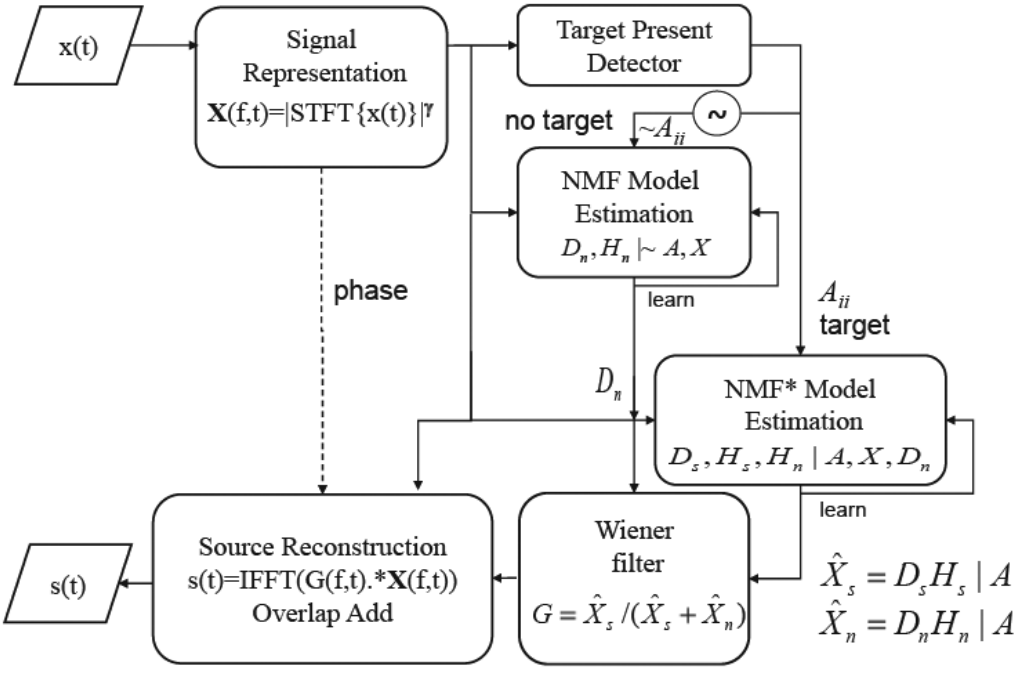

Fig. 1 - General scheme of the proposed signal enhancement framework.

and sparsity.

In the simplest case, NMF problem can be stated as follows: given a non-negative data matrix $\mathbf{X} \in \mathbb{R}_{+}^{F\times T}$ (with $x_{ft} \geq 0$ or equivalently $\mathbf{X} \geq 0$) and a reduced rank K ($K \leq min(F, T)$), find two non-negative matrices $\mathbf{D} \in \mathbb{R}_{+}^{F\times K}$, called dictionary and $\mathbf{H}$ $\mathbb{R}_{+}^{K\times T}$, called sparse code, which factorize $\mathbf{X}$ as well as possible, that is:

$$\mathbf{X} = \mathbf{DH} + \mathbf{E} \tag{1}$$

where $\mathbf{E} \in \mathbb{R}_{+}^{F\times T}$ represents the approximation error to minimize.

In this section, we describe the essential components of the one channel enhancement model developed for audio in Cabras *et al*. (2010b) and we show that they can be adopted to analyze single-sensor volcanic seismic datasets.

4.1. Source separation applied to single-channel volcanic signal

We aim to estimate the undesired components, or interference, *n(t)* and the target, *s(t)* directly from the observable data mix in the time domain, with minimal a priori knowledge. We assume that saturation effects are absent in the mixed observable *x(t)*:

$$x(t) = s(t) + n(t). \tag{2}$$

The existence of different superimposed independent signals that contribute to form volcanic

tremor at Erta 'Ale is discussed in Jones *et al*. (2012). This implies that in this case study it is reasonable to assume that *s(t)* and *n(t)* are uncorrelated. This extends linearity in the power spectral domain and let us transform the data in a non-negative representation suitable for NMF:

$$|\mathbf{X}(f, t)|^2 = |\mathbf{S}(f, t)|^2 + |\mathbf{N}(f, t)|^2 \quad (3)$$

where the observable signal *x(t)* is transformed into a complex time-frequency representation $\mathbf{X}(f, t)$. The proposed method is shown in Fig. 1 and key modules are discussed in the next subsections. This general single channel enhancement model is equivalent to the model presented in Cabras *et al*. (2010a) with a classical refiltering technique as suppression rule, such as a Wiener filter. A common technique to manipulate a time-varying observed signal consists of transforming it in a time-frequency representation that we describe in subsection 4.1.1. A priori knowledge about undesired components can be trained directly from selected time sections of the available signal using a NMF model estimation, which will be described in subsection 4.1.2. A further non trivial step is needed to assign the decomposed parts to the source of interest to discard the interference source; in subsection 4.1.3 we show how to solve this problem with a solution based on a constrained NMF (NMF*) model estimation and prior knowledge on undesired component.

4.1.1. Signal representation

We transform the signal into a time-frequency non-negative matrix energy representation (by a Short Time Fourier Transform - STFT) along time elements (frames) and frequency elements (bins). We represent the signal as an element-wise exponentiated STFT:

$$X = |STFT\{x(t)\}|^{\gamma} \quad (4)$$

The linearity expressed by Eq. (2) applies also to Eq. (4) when $\gamma = 2$, but even with seismic signals, our experimental results show that γ is an important parameter to NMF performance and $\gamma = 2$ is a bad choice for accurate component separation. To verify this important issue, we evaluated the results varying the value of γ on an empirically chosen range of values between 1/3 and 2. This experimental testing activity with Erta 'Ale and other volcanic tremor signals confirms previous component separation results adopting NMF in noisy speech enhancement by Schmidt *et al*. (2007) that an heuristic optimal choice is $\gamma = 2/3$, which corresponds to the cube root compression of power STFT, while outcomes are significantly worse using the power spectrogram representation ($\gamma = 2$).

4.1.2. Undesired component training

During the training stage, we assume availability of some target-absent frames, applying a human supervised selection, that we call Target Present Detection, to the observable signal $X(f, t)$; the resulting signal:

$$Z(f, t) = X(f, t)\, \bar{A}(t, t) \quad (5)$$

is equivalent to $X(f, t)$, with target-present frame suppressed by the diagonal index matrix $\bar{A}(t, t)$,

a binary square matrix showing the absence of target source in frame *t*:

$$\bar{A}(t,t)=\begin{cases}1, \text{ if target source is absent in frame t}\\ 0, \text{ otherwise.}\end{cases} \tag{6}$$

Applying a Regularized Euclidean NMF to $Z(f, t)$ (Eggert and Körner, 2004), we obtain the strictly positive dictionary $D_n(f, k)$ of the interference learned from data, where k is the number of user-defined elements of undesired component. Following the simplification proposed in Eggert and Körner (2004) to estimate the NMF model, we define as follows the complete multiplicative iterative algorithm (Cabras *et al*., 2010b):

1. initialize $D_n(f, k)$ and $H_n(k, t)$ with random values between 0 and 1, multiply $H_n(k, t)$ by $\bar{A}(t, t)$ to suppress target-present frames;
2. define Euclidean column-wise normalization of the dictionary to prevent joint numerical drifts in H_n and D_n:

$$\bar{D}_n(f,k)=\frac{D_n(f,k)}{\sqrt{\sum_f D_n(f,k)^2}}=\frac{D_n(f,k)}{\|D_n(K)\|_2} \tag{7}$$

3. calculate the reconstruction according to:

$$\hat{X}_n=\bar{D}_n H_n \tag{8}$$

4. update the sparse code according to the rule:

$$H_n \leftarrow H_n \bullet \frac{\bar{D}_n^T Z}{\bar{D}_n^T \hat{X}_n+\lambda_n} \tag{9}$$

5. calculate the reconstruction according the Eq. (8);
6. update the non-normalized dictionary according to the rule:

$$D_n \leftarrow \bar{D}_n \bullet \frac{ZH_n^T+\bar{D}_n \bullet \left(\mathbf{1}\left(\hat{X}_n H_n^T \bullet \bar{D}_n\right)\right)}{\hat{X}_n H_n^T+\bar{D}_n \bullet \left(\mathbf{1}\left(ZH_n^T \bullet \bar{D}_n\right)\right)} \tag{10}$$

7. repeat from step 2 until convergence to a local minimum of the Euclidean Cost function:

$$C^{(i)}=\frac{1}{2}\sum_{f,t}\left(Z(f,t)-\hat{X}_n(f,t)\right)^2+\lambda_n\sum_{k,t}H_n(k,t) \tag{11}$$

We stop the algorithm at iteration i when $|C^{(i)}-C^{(i-1)}| < \varepsilon C^{(i)}$.

Note that • operator indicates element-wise multiplication, the fraction line indicates element-wise division between two matrices, **1** is a suitable size square matrix of ones. Multiplicative rules ensure the non-negativity of the factor matrices, since all the successive estimates remain positive if the initial estimate is positive. The regularization parameter λ_n weights the importance of the sparsity term to the reconstruction.

The final D_n matrix represents the dictionary of the interference learned from data and it will be used by the next module to estimate the two additive sources composing the mixed signal.

4.1.3. Estimation of undesired source and target source

In order to estimate the sources, we use again an NMF* to compute the dictionary of the target source and the sparse code of both sources. Assuming, as usual, the additivity of sources, the dictionary of the mixed signal can be seen as the horizontal concatenation of the individual source dictionaries. Moreover, the sparse code of the mixed signal X can be seen as the vertical concatenation of the individual source sparse codes:

$$X = X_s + X_n = \left[D_s D_n\right]\begin{bmatrix} H_s \\ H_n \end{bmatrix} + E = DH + E. \tag{12}$$

In the previous Eq. (12), E is an unknown matrix representing approximation errors. We can not solve Eq. (12) directly with NMF, due to a permutation ambiguity. In fact, we can write

$$DH = (DP)(\mathrm{P}^{-1}H) \tag{13}$$

where P is a generalized permutation matrix, i.e., a matrix with only one non-zero positive element in each row and each column.

Schmidt *et al*. (2007) suggest to pre-compute D_n, as we have done in the previous section for the interference in the $Z(f, t)$ signal; then learn $D_s(f,m)$, $H_s(m, t)$ and $H_n(k, t)$, where m is the number of user defined elements of the target source, with a modified NMF*, which we apply to $Y(f, t) = X(f, t)A(t, t)$ (i.e., the observed signal in the target-present frames). We describe here the developed one-dictionary constrained (D^*_n) algorithm:

1. initialize $D_s(f,m)$, $H_s(m, t)$ and $H_n(k, t)$ with random values in the range (0÷1); to multiply $H_s(m, t)$ and $H_n(k, t)$ by A to suppress target-absent frames;
2. define Euclidean column-wise normalization of the target dictionary to prevent joint numerical drifts in H_s and D_s:

$$\bar{D}_s(f,m) = \frac{D_s(f,m)}{\sqrt{\sum_f D_s(f,m)^2}} = \frac{D_s(f,m)}{\left\|D_s(m)\right\|_2} \tag{14}$$

3. calculate the overall reconstruction according to:

$$\hat{X} = \bar{D}_s H_s + \bar{D}_n H_n \tag{15}$$

4. update the sparse code of target according to the rule:

$$H_s \leftarrow H_s \bullet \frac{\bar{D}_s^T Y}{\bar{D}_s^T \hat{X} + \ell_s} \tag{16}$$

5. calculate the overall reconstruction as in Eq. (15);
6. update the sparse code of interference according to the rule:

$$H_n \leftarrow H_n \bullet \frac{\bar{D}_n^T Y}{\bar{D}_s^T \hat{X} + \ell_n} \tag{17}$$

7. calculate the overall reconstruction as in Eq. (15);
8. update the target non-normalized dictionary according to the rule:

$$D_s \leftarrow \bar{D}_s \bullet \frac{YH_s^T + \bar{D}_s \bullet \left(1\left(\hat{X}H_s^T \bullet \bar{D}_s\right)\right)}{\hat{X}H_s^T + \bar{D}_s \bullet \left(1\left(YH_s^T \bullet \bar{D}_s\right)\right)} \tag{18}$$

9. repeat from step 2 until it reaches the convergence of the Euclidean Cost function to minimize:

$$C^{(i)} = \frac{1}{2}\sum_{f,t}\left(Y(f,t) - \hat{X}(f,t)\right)^2 + \ell_n \sum_{k,t} H_n(k,t) + \ell_s \sum_{m,t} H_s(\boldsymbol{m},t). \tag{19}$$

We stop the algorithm at iteration i when $|C^{(i)} - C^{(i-1)}| < \varepsilon C^{(i)}$. The regularization parameters ℓ_s and ℓ_n determine the degree of sparsity in the activity matrix. D_n, the dictionary of the undesired component, is left unchanged by this algorithm because it is predefined and fixed by the previous training stage; moreover, we do not seek a sparse code for the fixed dictionary, but the code that minimizes the reconstruction error, setting $\ell_n = 0$. In general λ_n, ℓ_s, k and m are depending on unknown sources, i.e., are defined a priori.

5. A case study: Erta 'Ale convection regimes

For illustrative purposes, we applied our methodology to a seismic dataset recorded at Erta 'Ale volcano, where the target is defined to be the seismic footprint of the fast convective regime while the interference is defined to be the tremor associated to the slow convective regime. The seismic footprints of each regime were identified by comparison of spectral patterns with direct

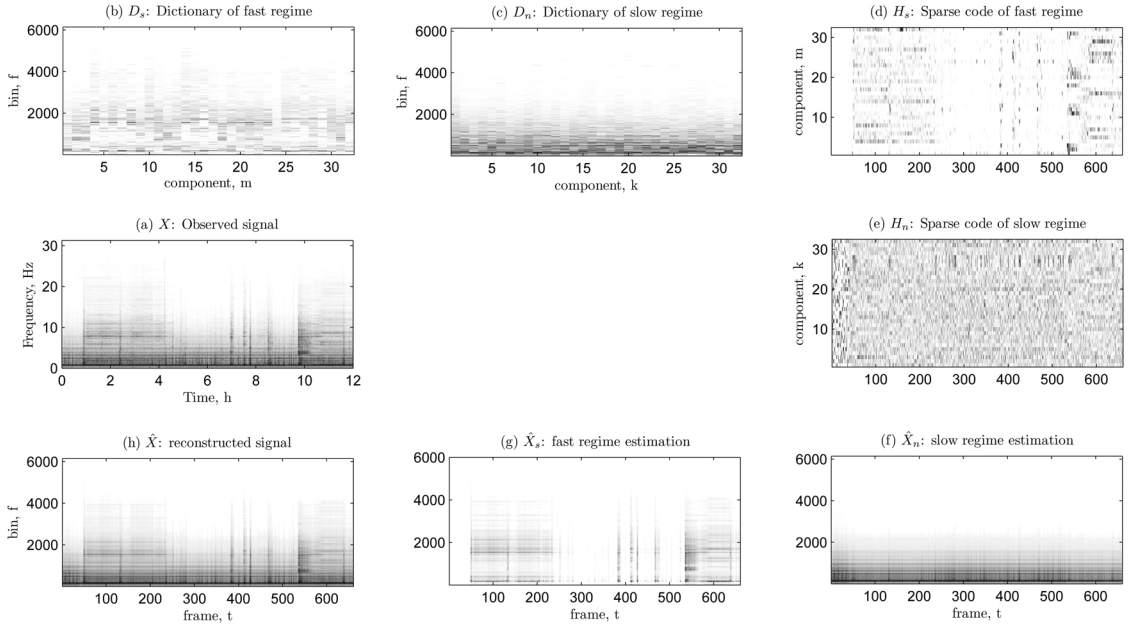

Fig. 2 - Matrices involved in sources estimate. a) In the 12 hours spectrogram registration, we recognize continuous tremor with spectral changes corresponding to the changes in the rate of lava lake convection; b) dictionary of target as learned by target component estimate in target-present frames, in this case the target is the fast regime; c) dictionary of interference D_n as trained by undesired component estimate in target-absent frames, in this case the interference is the slow regime; d) the fast regime sparse code and e) the slow regime sparse code; f) interference estimate, i.e., slow regime; g) target estimate, i.e., fast regime; h) overall signal reconstruction which is comparable to observed signal (a).

observations and video recordings (Harris *et al*., 2005; Jones *et al*., 2006). As argued by Harris (2008) and Jones (2009), tremor recorded during the "fast" convective regime appears to be new signals superimposed on the background signals of the "slow" convective regime. The examples of slow regime to train the dictionary of interference were identified manually on the base of visual observations. With our experimental datasets, good results were obtained for $\lambda_n = 0.2$ and $\ell_s = 0.05$, $k = 32$ and $m = 32$.

Fig. 2 shows the matrices modeling the involved target and interference estimations of Eq. (12). It is worth noting that the dictionary of interference [panel (c)] was trained in the previous stage and kept fixed in this separation stage.

The resulting fast regime spectrogram $\hat{X}_s = D_s H_s$ estimate and the slow regime spectrogram $\hat{X}_n = D_n H_n$ estimate are shown in Fig. 3.

6. Conclusions

NMF techniques can be used to separate different components of volcanic origin which are superimposed in time and frequency and the source of interest is non-stationary, as shown at Erta 'Ale single-sensor case study. In this case, the separation of sources is not blind as in ICA applications (Cabras *et al*., 2010c), because the learning algorithm of NMF requires "background

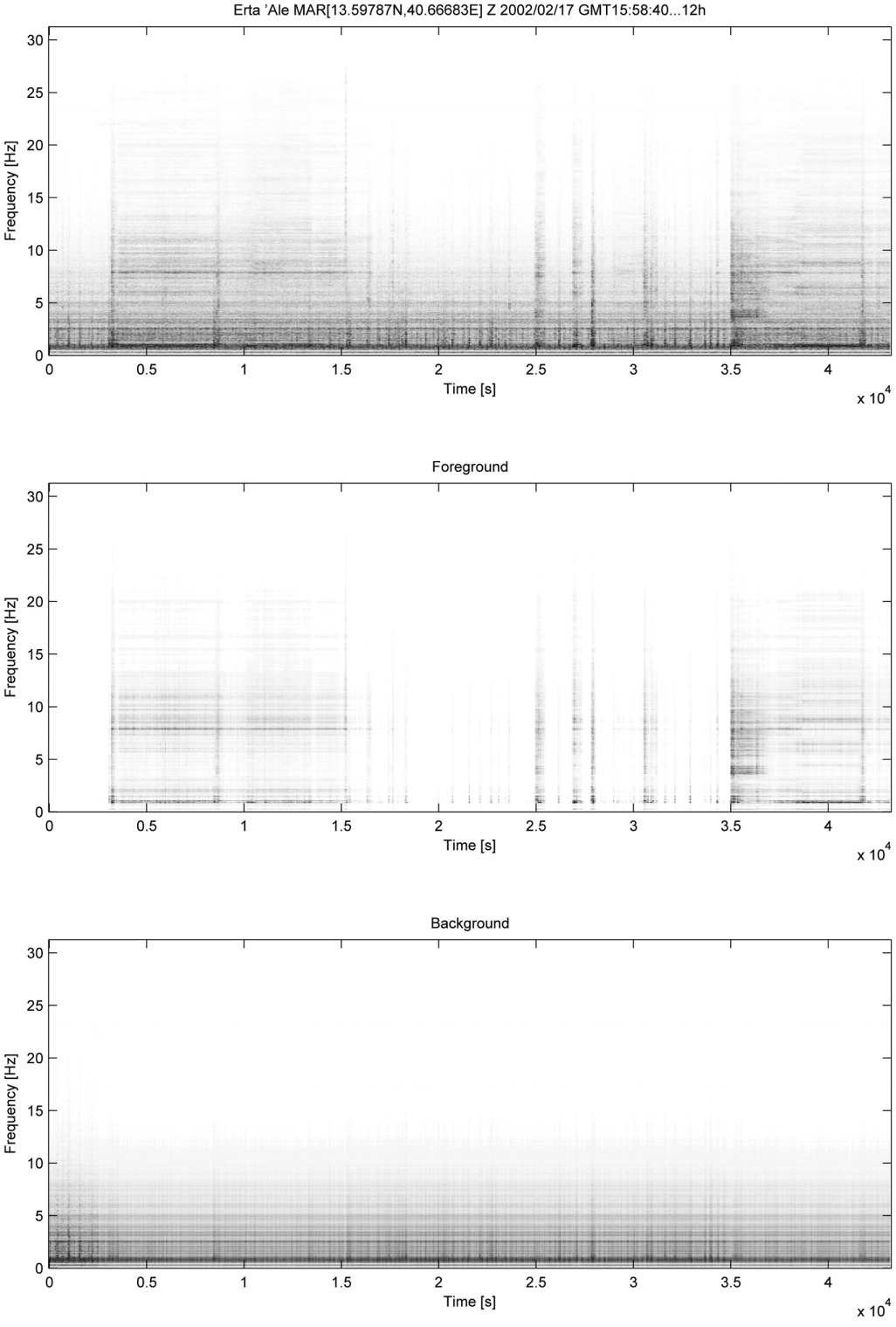

Fig. 3 - Spectrograms of original corrupted signal X (top panel), estimated target source $\hat{X}_s$ (center panel) and estimated interference $\hat{X}_n$ (bottom panel) of 12 hours of Erta 'Ale Z component MARS seismometer. Slow regime pattern (bottom) and fast regime pattern (center) are clearly separated.

samples" but, acting on a single channel, can have wider applicability, particularly because most volcanoes have only limited seismic monitoring. The subtle changes associated with the departure of volcanic tremor from background signal regimes could be detected by such algorithms, which could lead to better early detection of unrest. The example here demonstrates that, even with only one seismic station, NMF can help to explore fundamental questions about the nature and causes of volcanic tremor. In particular, the proposed technique can assume an important role in the efficient filtering of low signal-to-noise volcanic seismic data by extracting coherent volcanic components from more energetic background noise. Presumably, this method could be applied almost identically to other volcanoes whose tremor exhibits similar spectral transitions, e.g., Ambrym (Carniel *et al*., 2003) or Stromboli (Ripepe *et al*., 2002). Moreover, it could potentially be extended to the extraction of tremors of other origin [e.g., geothermal in Carniel *et al*. (2010) or plate subduction in Rogers and Dragert (2003)] which are often characterized by a low signal-to-noise ratio, and to the proper analysis of seismic noise with important seismic risk implications [such as site effects estimation with HVSR (Carniel *et al.,* 2006)] and/or clear economic implications [such as the identification of hydrocarbon tremor (Ali *et al*., 2010)]. The theoretical limit of the proposed signal enhancement model, depicted in Fig. 1, is given by the combination of the modified spectral amplitude (refiltered with a simple Wiener rule) and the unmodified noisy observed phase. An enhancement of the phase could be desirable at low SNR, although phase enhancement is an open problem without strong hypotheses concerning the unknown target.

Acknowledgements. The analyzed data set was collected in the framework of a joint project by Universities of Udine, Washington and Hawaii. Istituto Nazionale di Oceanografia e di Geofisica Sperimentale-CRS: Centro di Ricerche Sismologiche, Udine (Italy) provided MARS seismic station. Comments by anonymous reviewers helped to improve the manuscript.

REFERENCES

Alean J., Carniel R. and Fulle M.; 2011: *Stromboli online, volcanoes of the world, information on Stromboli, Etna and other volcanoes.* http://stromboli.net.

Ali M.Y., Berteussen K.A., Small J. and Barkat B.; 2010: *Low-frequency passive seismic experiments in Abu Dhabi, United Arab Emirates: implications for hydrocarbon detection.* Geophys. Prospect., **58**, 869-893.

Barberi F. and Varet J.; 1970: *The Erta Ale volcanic range.* Bull. Volcanol., **34**, 848-917.

Cabras G., Canazza S., Montessoro P.L. and Rinaldo R.; 2010a: *Restoration of audio documents with low SNR: a NMF parameter estimation and perceptually motivated Bayesian suppression rule.* In: Proc. Sound and Music Computing Conference, Barcelona, Spain, pp. 314-321.

Cabras G., Canazza S., Montessoro P.L. and Rinaldo R.; 2010b: *The restoration of single channel audio recordings based on non-negative matrix factorization and perceptual suppression rule.* In: Pomberger H., Zotter F. and Sontacchi A. (eds), Proc. 13th Int. Conf. Digital Audio Effects DAFx-10, Graz, Austria, pp. 458-465.

Cabras G., Carniel R. and Wassermann J.; 2008: *Blind source separation: an application to the Mt. Merapi Volcano, Indonesia.* Fluctuation Noise Lett., **8,** L249-L260.

Cabras G., Carniel R. and Wassermann J.; 2010c: *Signal enhancement with generalized ICA applied to Mt. Etna Volcano, Italy.* Boll. Geof. Teor. Appl., **51**, 57-73.

Carniel R., Barazza F. and Pascolo P.; 2006: *Improvement of Nakamura technique by singular spectrum analysis.* Soil

Dyn. Earthquake Eng., **26**, 55-63.

Carniel R., Di Cecca M. and Rouland D.; 2003: *Ambrym, Vanuatu (July-August 2000): spectral and dynamical transitions on the hours-todays timescale.* J. Volcanol. Geotherm. Res., **128**, 1-13.

Carniel R., Jolis E.M. and Jones J.; 2010: *A geophysical multi-parametric analysis of hydrothermal activity at Dallol, Ethiopia.* J. Af. Earth Sci., **58**, 812-819.

Carniel R., Tarraga M., Barazza F. and Garcia A.; 2008: *Possible interaction between tectonic events and seismic noise at Las Canadas volcanic caldera, Tenerife, Spain*. Bull. Volcanol., **70**, 1113-1121.

Dainelli G. and Marinelli O.; 1907: *Vulcani attivi della Dancalia.* Riv. Geog. Ital., **13**, 261-270.

Dangel S., Schaepman M., Stoll E., Carniel R., Barzandji O., Rode E. and Singer J.; 2003: *Phenomenology of tremor-like signals observed over hydrocarbon reservoirs*. J. Volcanol. Geotherm. Res., **128**, 135-158.

Eggert J. and Korner E.; 2004: *Sparse coding and NMF.* In: Proc. Int. Joint Conf. on Neural Networks, Budapest, Hungary, vol. 2, pp. 2529-2533.

Harris A.; 2008: *Modelling lava lake heat loss, rheology, and convection.* Geophys. Res. Lett., **35**, L07303.

Harris A., Carniel R. and Jones J.; 2005: *Identification of variable convective regimes at Erta Ale lava lake.* J. Volcanol. Geotherm. Res., **142**, 207-223.

Jones J.; 2009: *Subband analysis of continuous volcanic tremor.* PhD Thesis, Univ. Washington, Seattle, WA, USA.

Jones J., Carniel R., Harris A.J.L. and Malone S.; 2006: *Seismic characteristics of variable convection at Erta Ale lava lake, Ethiopia.* J. Volcanol. Geotherm. Res., **153**, 64-79.

Jones J., Carniel R. and Malone S.; 2012: *Decomposition, location, and persistence of seismic signals recovered from continuous tremor at Erta 'Ale, Ethiopia.* J. Volcanol. Geotherm. Res., **213-214**, 116-129, doi:10.1016/j.jvolgeores.2011.07.007.

Kadota T. and Labianca F.; 1981: *Gravity-wave induced pressure fluctuations in the deep ocean.* IEEE J. Oceanic Eng., **6**, 50-58.

Konstantinou K. and Schlindwein V.; 2002: *Nature, wavefield properties and source mechanism of volcanic tremor: a review.* J. Volcanol. Geotherm. Res., **119**, 161-187.

Lee D.D. and Seung H.S.; 1999: *Learning the parts of objects by non-negative matrix factorization.* Nature, **401**, 788-791.

Lovallo M., Telesca L. and Carniel R.; 2010: *Timedependent fisher information measure of volcanic tremor.* J. Volcanol. Geotherm. Res., **195**, 78-82.

Oppenheimer C. and Francis P.; 1998: *Implications of longeval lava lakes for geomorphological and plutonic processes at Erta 'Ale volcano, Afar.* J. Volcanol. Geotherm. Res., **80**, 101-111.

Ripepe M., Harris A.J.L. and Carniel R.; 2002: *Thermal, seismic and infrasonic evidences of variable degassing rates at Stromboli Volcano.* J. Volcanol. Geotherm. Res., **118**, 285-297.

Rogers G. and Dragert H.; 2003: *Episodic tremor and slip on the cascadia subduction zone: the chatter of silent slip.* Science, **300**, 1942–1943.

Schmidt M.N., Larsen J. and Hsiao F.T.; 2007: *Wind noise reduction using non-negative sparse coding.* In: Proc. IEEE Workshop on Machine Learning for Signal Processing, Thessaloniki, Greece, pp. 431-436.

Corresponding author: Giuseppe Cabras
Dipartimento di Chimica, Fisica e Ambiente (DCFA), Università di Udine
Via del Cotonificio 108, 33100 Udine, Italy
Phone: +39 0432 558212; fax: +39 0432 558222; e-mail: giuseppe.cabras@uniud.it